COMPLEX REFLECTION COEFFICIENTS OF WATER WAVES

ON THE CLASSIFICATION OF TYPES OF BREAKERS

FRITZ BÜSCHING

Bielefeld University of Applied Sciences, Germany,
Dießelhorststr. 1, 38116 Braunschweig, buesching@hydromech.de

Abstract

Based on lab investigations, specific phenomena of waves breaking on rather steep slopes (1:2 and 1:3) are traced back partly to varying phase shifts $\Delta\varphi$, occurring between incident and reflected waves. As an analogue of electromagnetic waves at uniform planar interfaces, the process of wave breaking is regarded as combined effects resulting from reflection, transmission and dissipation. Accordingly a *complex reflection coefficient* Γ (CRC) is defined comprising of the magnitude $C_r = H_r/H_i$ and the phase $\Delta\varphi$. Results are presented by magnitudes and phases for irregular waves in the complex number plane and for monochromatic waves with reference to some frequencies and slope angles. As the CRC phase angle controls the positioning of the partial standing wave and thus the location of the breaker depth at a slope, it should be considered for the classification of breakers.

1. Introduction

The effects of breaking waves are decisive for the design of coastal structures. As far as sloping structures are concerned, the breaker number ξ also termed Ir (after Iribarren, 1949), has proved to be the most useful parameter.

$$\xi = \tan\alpha/\sqrt{(H/L)} \qquad [1]$$

Its variables are the slope angle $\tan\alpha$ = 1:m , wave height H and wave length L.
As is well known, this parameter is used not only for classifying the different types of breakers but also for describing the reflectivity of structures by using the ratio of reflected wave height divided by incident wave height (H_r/H_i), which normally is termed reflection coefficient.
By contrast the effect of *phase shifting* γ between incident and reflected wave, presumed already by Schoemaker and Thijsse (1949) [1], did not draw very much attention. The author, however, had come across this phenomenon, when investigating breaking waves on different revetment structures producing a phase jump $\Delta\varphi$ [3], [4].
Previously Sutherland and O´Donoghue (1998) [2] analyzed the state of knowledge from about 20 references complementing it by their own experiments. Using an extensive experimental data set, involving normal incident and oblique incident regular and irregular waves, they arrived at the conclusion that the phase shift γ is uniquely determined by a nondimensional number χ_3 defined by structure slope $\tan\alpha$ = 1:m, water depth at the structure toe d_t , wave period T, and angle of incidence θ.

$$\chi_3 = \chi\sqrt{\cos\theta} = \frac{1}{\tan\alpha}\sqrt{\frac{d_t\cos\theta}{gT^2}} \qquad [2]$$

For instance, the best-fit line for 3-D irregular waves is given as follows:

$$\gamma = -11.13\cdot\pi\cdot\chi_3^{1,41}. \qquad [3]$$

Accordingly neither the wave height nor energy dissipation processes should influence the phase shift, with the consequence that such quantities were irrelevant for the description of breaking waves too.

The author, however, has arrived at more differentiated results, regarding the *breaking process of waves at rather steep sloping structures* in such a way that a variable phase difference $\Delta\varphi$ between the incident and reflected wave plays an important part in the reflection process[3], [4].

In the author's view not only the phenomena of *reflection* and *dissipation* have to be considered for describing the wave breaking process, but *transmission* too; just like an analogue of electromagnetic waves at uniform planar interfaces: In the course of the dissipating wave breaking process, a wave pulse of transmission evolves from the initial incident wave at the landward side, while a reflected wave is produced on the seaward side at the same time. The wave pulse of transmission is characterized by a wave height $H_t < H_i$ and phase velocity $c_t < c_i$, and the reflected wave height is $H_r < H_i$.

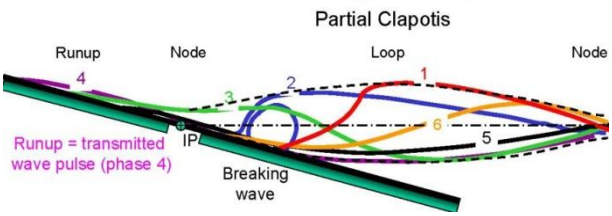

Figure 1: Six phases of a plunging breaker at the condition of a phase jump, caused by partial reflection and by the transmitted pulse of wave run up. In phases 3 and 4, there are opposite water level movements (flipping deflections) at both sides of the imperfect Clapotis node nearly coinciding with IP.

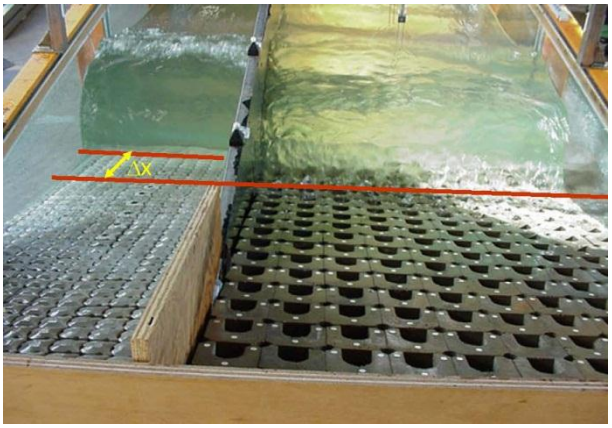

Figure 2: Plunging breaker at quasi smooth reference revetment slope (left) and collapsing breaker at hollow slope structure (right). Varying distances (Δx) between breaker front faces indicate modified phase shifts between incident and reflected waves.

In this process it is essential that due to the conservation of momentum, the positive water level deflection of the transmitted wave pulse postulates locally a negative water level deflection of the reflecting wave. Hence, the superimposition of incident and reflected waves results in a partially standing wave comprising of a phase jump $\Delta\varphi$. The partial Clapotis node close to the point IP, where the structure front face intersects the still water level, can be regarded as a center of elliptical movement, around which the water level deflections of the washing movement (runup – rundown) and those of the partial standing wave occur in opposite (flipping) phases, see Figure 1.

Especially with respect to plunging breakers and collapsing breakers, it can be presumed that the particle movement in an imperfect node near IP attributes to the formation of circularly shaped breaker eddies.

The trigger of the author´s above considerations is due to the findings, derived from wave tank tests executed on *hollow* concrete elements in the wave tank of Bielefeld University of Applied Sciences (BUAS) in the 1990ies, see Fig.2.

Especially it had come out from such tests of scale 1:5 that by means of appropriate interference with the washing movement not only the wave run-up and the breaker height could significantly be reduced, but also the *breaker type* and its *relative position* on the slope face was modified [5].

In the following the results presented in [3] and [4] concerning the occurrance of a phase jump, will be partly extended and modified respectively. Therefore instead of defining the reflection coefficient as a function of two variables $C_r = f(H_r/H_i, \Delta\varphi)$, at this place it will be defined as a *complex quantity* $\Gamma = C_r e^{i\Delta\varphi}$, which appears to be the more appropriate option.

For the time being, however, relations to the results of the above mentioned studies (Sutherland und O´Donoghue (1998) [2]) cannot be made, because in the present assessment

- the point IP of the still water level intersecting the slope face is selected as the point of reference and thus the phase shift here is $\Delta\varphi \neq \gamma$,
- the investigations are restricted to the 2-dimesional retro-reflection from 4 (2 x 2) steep slopes only,

- contrary to above presumptions essential importance is attached to the interactions between phase shift and energy dissipation at wave breaking and
- absorption at sloping structures is assumed to be not only represented by a smaller reflecting wave height $H_r < H_i$ but also is accompanied by a modified phase shift $\Delta\varphi$ between incident and reflected wave.

2. Mathematical pre-examinations

In the general case of regular monochromatic waves the mathematical formulation of the incident wave with amplitude A can be given as follows:

$$y(x,t) = A\cos(\omega t - kx) = Re[A\cos(\omega t - kx) + i\,A\sin(\omega t - kx)]$$

$$= Re\left[Ae^{i(\omega t - kx)}\right] = Ae^{i(\omega t - kx)} \qquad [4]$$

where the angular frequency $\omega = \frac{2\pi}{T}$ and the wave number is $k = \frac{2\pi}{L}$.

These are both the *cosine* and the *complex* formulations respectively.
Note that according to conventional rules, the Re[ ]-operator is not written.

The expression of the reflected wave results from the incident wave by multiplying the later by the reflection coefficient and thereby accounting for a phase shift $\Delta\varphi$. Moreover a negative sign has to be used at the wave number, because the reflected wave moves in the opposite direction.
If the place of reflection is supposed to be at x=0, which is located at the right hand side, the wave activity is in the negative range and the description of the reflected wave is as follows:

$$y(x,t) = C_r A\cos(\omega t + kx + \Delta\varphi) = C_r \cdot Ae^{i(\omega t + kx + \Delta\varphi)}$$

$$= (C_r e^{i\Delta\varphi}) \cdot Ae^{i(\omega t + kx)} = \Gamma \cdot Ae^{i(\omega t + kx)} \qquad [5]$$

According to equation [5] capital gamma Γ is defined as a *complex reflection coefficient (in short: CRC)*, i.e. complex reflected wave devided by the complex incident wave, - related to x = 0

$$\Gamma = C_r e^{i\Delta\varphi} \qquad [6]$$

where $C_r = H_r/H_i$ is the wave height ratio and
$\Delta\varphi$ is the phase shift between the reflected and the incident wave at the point of reflection.

It shall be noted here that differing from signal transmission technology, at this place $\Delta\varphi$ is used instead of the mere angle φ .
Defining the reflection coefficient as a complex quantity - e.g. as an analogue to the composition of the impedance in an AC-circuit - one can distinguish between

- the total reflection coefficient (magnitude and phase; to be compared with the *impedance*),
- its real part (to be compared with the *resistance*) and
- its imaginary part (to be compared with the *reactance (capacitive and inductive)*).

Consequently the total wave field can be formulated by summing up equations [4] and [5] in the cosine formulation as

$$y(x,t) = A\cos(\omega t - kx) + C_r A\cos(\omega t + kx + \Delta\varphi) \qquad [7]$$

and in the polar complex vector presentation as

$$y(x,t) = Ae^{i(\omega t - kx)} + C_r Ae^{i(\omega t + kx + \Delta\varphi)} = (e^{-ikx} + C_r e^{i\Delta\varphi} e^{ikx}) Ae^{i\omega t}$$

$$= (e^{-ikx} + \Gamma\, e^{ikx}) Ae^{i(\omega t)} \qquad [8]$$

Besides other purposes equation [8] also forms the basis for the design of electronic communication devices. Its evaluation gives the following two special cases of total reflection:

A. Positive total reflection

$$y(x,t) = (e^{ikx} + e^{-ikx}) Ae^{i\omega t} = 2\, A cos\, kx\, e^{i\omega t} \qquad [9]$$

where $\Delta\varphi = 0°$ and $C_r = 1$, then $\Gamma = 1$.
This is the equation of a perfect standing wave (Clapotis) without phase jump.

B. Negative total reflection

$$y(x,t) = (e^{-ikx} - e^{ikx}) Ae^{i\omega t} = -2\, i\, A sin\, kx\, e^{i\omega t} \qquad [10]$$

where $\Delta\varphi = 180°$ and $C_r = 1$, then $\Gamma = -1$.
This is also the equation of a perfect standing wave, however, with a phase jump of 180° (π) between incident and reflected wave. This Clapotis is, however, shifted in position with reference of the former by L/4 and in phase by 90°.

As is well known, both cases also appear approximately when generating standing rope waves in a single vertical plain. If the rope is not fixed at its rear end in the vertical direction, there is positive total reflection, whereas negative total reflection exists, if the rope is fixed at the rear end in both vertical and horizontal directions.

Besides the presentation in phasor diagrams (see Fig.11 and 12 below) the properties of complex reflection coefficients can also be clarified by using parametrical presentations.
In Fig.3, for instance, the real part Re[Γ] of magnitudes $0.1 \le Cr = H_r/H_i \le 1.0$ and phase angles $0° \le \Delta\varphi \le 180°$ can be read from the vertical axis. Outside this range, reflection coefficients can be found by mirroring the data at the vertical axis through $\Delta\varphi$=0° and at the vertical axis through $\Delta\varphi$=180° respectively.
It is important to note that there are negative reflection coefficients for phase shifts $90° < \Delta\varphi < 270°$, $450° < \Delta\varphi < 630°$, ….

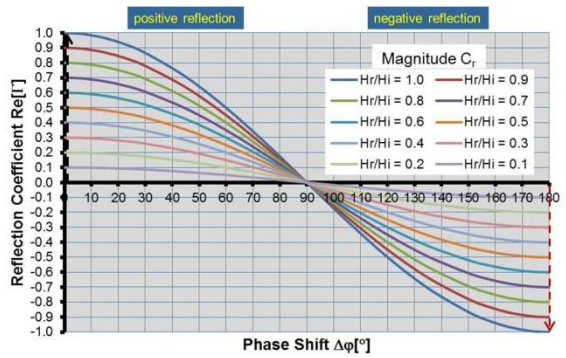

Figure 3: Real part Re[Γ] of magnitudes $0.1 \le Cr = Hr/Hi \le 1.0$ and phase angles $0° \le \Delta\varphi \le 180°$ (of the complex reflection coefficient Γ.)

Considering at first the theoretical case of equal cosine wave heights $H_i = H_r$ (curve parameter $H_r/H_i = 1$), the real part Re[Γ] = 1.0 at $\Delta\varphi = 0°(\pm n*360°)$ is attached to a perfect Clapotis comprising of a loop at the point of reflection (as e.g. at a vertical wall), cf. equation [9]. Contrary $\Delta\varphi = 180°$ ($\pm n*360°$) delivers Re[Γ] = -1.0 according to equation [10]. The later, however, also stands for a perfect Clapotis, but in this case with a perfect node existing at the point of reflection and thus a phase jump is produced.

Considering both of the Clapotis waves separately apart from their originating incident and reflected waves, their loops (and nodes respectively) appear shifted by an angle of $\Delta\psi$ = 90° (π/2). Accordingly for $\Delta\varphi$ changing from 0° to 180°, the transfer from the case of reflection *without* phase jump to the case of reflection *with* phase jump can be watched; the later meaning that the wave crest is reflected as a wave trough and vice versa.

Phase differences $-90° < \Delta\varphi < 0°$, $0° < \Delta\varphi < 90°$, $90° < \Delta\varphi < 180°$ and $180° < \Delta\varphi < 270°$, however, represent *partial* standing waves, which can be considered a mixture of progressive and standing waves. In those cases imperfect nodes are located at distances $0 < a_i < L_i/4$ from IP. Of course there are also partial standing waves at phase differences $0°$ ($\pm$ n*360°) and $180°(\pm$ n*360°), if parameter $H_r/H_i < 1$.

According to the theory of propagating *signals on electric power lines*, there also will exist partial reflections on the later, if the terminating resistor Z_a differs from the cable's characteristic impedance Z_w. Hence, the above mathematical approach also applies in that case, in which, however, the complex reflection coefficient normally is characterized by r, |r| and φ instead of Γ, C_r and $\Delta\varphi$.

Provided that there are *sinusoidal* signals on *homogeneous* electric lines without any damping effects, the following 3 special cases of complex reflection coefficients can be distinguished:

No-load case (open loop with terminating resistor $Z_a = \infty$): $r = \Gamma = +1$, $|r| = C_r = 1$, $\varphi = \Delta\varphi = 0°$,
Matching case (no reflections because of $Z_a = Z_w$): $r = \Gamma = 0$, $|r| = C_r = 0$ and
Short circuit case (short circuited end of the line $Z_a = 0$): $r = \Gamma = -1$, $|r| = C_r = 1$, $\varphi = \Delta\varphi = 180°$

In this list it is, however, striking that usually no special phase angle is stated for the *matching* condition. On the other hand exactly such a case of *no reflection* in terms of the author´s definition $C_r = f(H_r/H_i, \Delta\varphi)$ in [3] und [4] is found for $\Delta\varphi = 90°$. Hence, the definition of $C_r = f(H_r/H_i, \Delta\varphi)$ can be named a reflection coefficient *sui generis*, whereas the *complex reflection coefficient (CRC)* $\Gamma = C_r e^{i\Delta\varphi}$ is the *complete* definition instead of the application of the mere *wave height ratio* H_r/H_i .

3. Experimental Procedure for the Determination of Complex Reflection Coefficients

As is well known from other kinds of waves, reflection coefficients can be determined from measurements on the wave field. In the case of water waves, however, until recently the structure of Healy´s formula (1953) was used for the determination of the *magnitude* of the reflection coefficient only, see Fig.4.

$$C_r = \frac{H_{\max} - H_{\min}}{H_{\max} + H_{\min}} \qquad \text{where } H_{\max} = H_i + H_r \text{ and } H_{\min} = H_i - H_r \qquad [11]$$

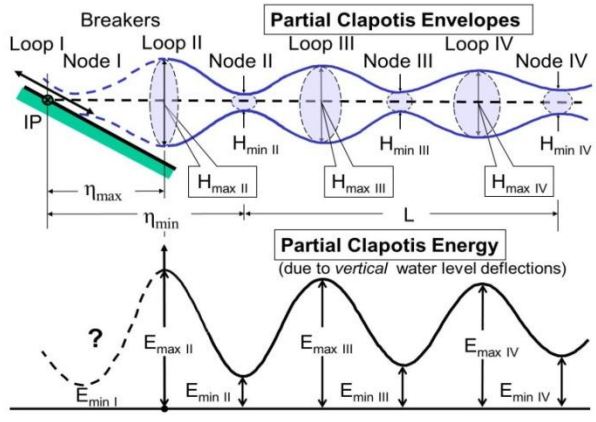

Figure 4. Sketch of water level envelopes derived from the potential energy of a partial standing wave at a slope, based on wave energy spectrum measurements at BUAS-Laboratory since 1992.

In this equation the quantities H_{max} and H_{min} refer to the vertical distances of the partial Clapotis envelopes shown in the upper part of Figure 4.
In the case of irregular waves, the author, however, since 1992 keeps on using the following formula [12], which is modified from Healy´s in such a way that the sums and differences of the wave heights of formula [11] had been substituted by the square roots of the energy´s extreme values, to be taken from the lower part of Figure 4.

$$C_{r,i} = \frac{\sqrt{E_{\max,i}} - \sqrt{E_{\min,i}}}{\sqrt{E_{\max,i}} + \sqrt{E_{\min,i}}} \quad . \qquad [12]$$

where:
$E_{max,\,i}$= maximum energy of contributing frequency components at clapotis node i,
$E_{min,\,i}$ = minimum energy of contributing frequency components at clapotis node i,
i = ordinal number of partial clapotis loops or nodes respectively.

With respect to the phase shift $\Delta\varphi$, however, *hardly any analysis* of extensive water level deflections of partial standing waves had been executed, since Mansard and Funke (1980) [12] had introduced their 3-point method for separating irregular incident and reflected waves.
Besides the above maximum and minimum water level deflections (H_{max}, H_{min}, equation [11]) or values of energy respectively, especially for the determination of the reflection coefficient´s *phase (CRC Phase),* additionally the wave *length L* and the *distance* η between the effective reflection point and an (imperfect) loop or node (respectively) are needed, see Fig. 4
In the case that the distance between the reflection point and the nearest loop is known, the phase of the reflection coefficient can be found from the following consideration.

Assuming a spot at a distance η from the reflection point, the phase shift for the incident wave to travel from here up to the point of reflection is $k\eta = 2\pi(\eta/L)$. At the point of reflection the (unknown) phase shift $\Delta\varphi$ appears and the *reflected* wave needs another $k\eta$ to return to the initial spot.

Thus at this spot, the total phase difference between incident and reflected wave has summed up to yield $2k\eta + \Delta\varphi$. At the condition of a loop existing at the respective spot, this phase difference must be an integer multiple of 2π, in order that incident and reflected waves superimpose to give maximum water level deflections.
Hence this can be put in the following equation

$$2k\,\eta_{max} + \Delta\varphi = n \cdot 2\pi \qquad [13]$$

With n = 1 for the nearest loop to the reflecting structure, this equation can be solved for the phase angle $\Delta\varphi$ of the reflection coefficient:

$$\Delta\varphi = 2\pi - 2k\,\eta_{max} \qquad respectively$$

$$\Delta\varphi[^\circ] = 360\left(1 - \frac{2\,\eta_{max}}{L}\right) \qquad [14a]$$

With regard to the condition of a node, the respective phase difference must be equal to an odd integer multiple of 180° (π), in order that incident and reflected waves tend to cancel. Hence the analogue formula is

$$\Delta\varphi[^\circ] = 180\left(1 - \frac{4\,\eta_{min}}{L}\right) \qquad [14b]$$

As to the analysis of irregular waves the author, however, did not directly refer to the wave field (water level envelopes), but principally to the quadratic values of the water level deflections, represented by the energy plotted – in principle - in the lower part lower part of Fig.4.
In [3] and [4] it had been explained in detail that such values are based on the integration of composite energy spectra, representing the water level deflections of incident and reflected waves (and possibly re-reflected waves) at any measuring station.
In Fig. 5 there are shown such values of all the integrated spectra belonging to the revetment configurations of Fig.2, plotted along with the gauge station distance from the slope face, i.e. from the point IP of the still water level intersecting the slope face.
With respect to the *total* analyzed frequency range $0.0326\text{Hz} \le f \le 1.3997\text{Hz}$ a *periodic* feature can be noticed yet in the upper red curve, belonging to the potential energy data calculated for the smooth sloping structure. This feature is fairly obvious, although there are noise effects contained in the frequencies f > 0.8Hz. By this reason it apparently confirms the existence of a partial standing wave, whose potential energy – contrary to that of a progressive wave – keeps on location. Its wave length

of about L_C = 3.65m for instance can be taken from the graph to be equal to the distance between the second and the forth minimum of energy and the first minimum of Energy E_{min} corresponding to the first node can be extrapolated close to IP.

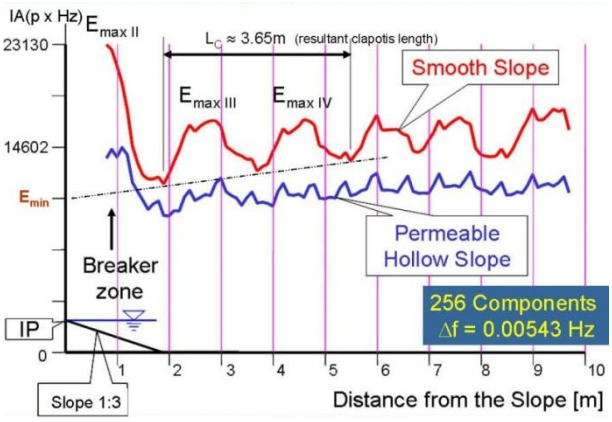

Figure 5: Integral values of spectral energy within the total frequency range 0.03 Hz ≤ f ≤ 1.4 Hz, documenting the existence of a partial Clapotis in front of the smooth slope 1:3. Extrapolated minimum E_{minI} is close to IP.

The general properties of partial waves, presented in the BUAS wave tank, can be derived from their energy distribution in the length expansion (energy line) as shown in Fig.04. In the lower part of that graph, it can be seen that the absolute maximum of energy (denoted E_{maxII}) appears closest to the slope and the seaward maxima E_{maxIII}, E_{maxIV} …decrease in magnitude with the distance increasing from the slope. Vice versa with respect to the *curve minima* the energy increases with distance from the slope in the order E_{minII}, E_{minIII}, E_{minIV} … This also applies for re-reflected waves in the wave tank used.

Such features evidently correspond rather well to the water level envelopes of a partial standing wave, shown in the upper part of Fig.04.

Differing from the periodical potential energy function of a *perfect* standing wave (Clapotis at a vertical wall), at which the nodes are related to zero values and the loops to maximum values, at partial standing waves the respective extreme values distinctively deviate from that periodical function.

With respect to magnitude and phase of the complex reflection coefficient such differences may be demonstrated schematically by a pair of standing waves of different wave lengths L_o, L_i in Figure 6.

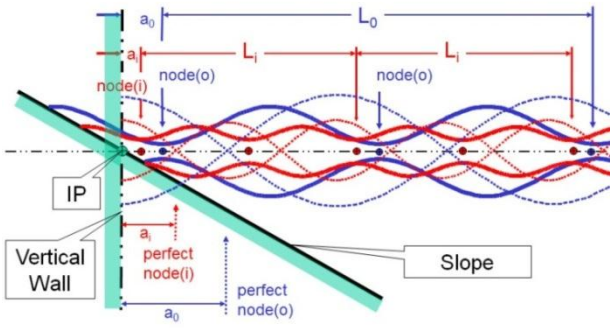

Figure 6: Two sets of partial standing waves of lengths L_o and L_i at a vertical wall and at a slope. Vertical wall: dotted lines; Smooth slope: solid lines.

Because of the vertical boundary missing, in those cases the perfect nodes convert into approximately elliptical flow lines (spiral shaped imperfect nodes), whose centers are located appreciably nearer to IP than L/4, 3L/4, 5L/4 …

Contrary to the perfect nodes of standing waves (L_o, L_i) at distances $a_0 = L_0/4$ and $a_i = L_i/4$ respectively from a vertical wall, the imperfect nodes at steep slopes get closer to IP the shorter they are (the higher their frequencies are)[4], [5].

As will be shown by equation [15], see below, such a reduction is equivalent to an *increase* of the phase information $\Delta\varphi$ of the complex reflection coefficient. At the same time there is a reduction of the magnitudes $C_r = H_r/H_i$ of the complex reflection coefficient proceeding with decreasing wave lengths.

Furthermore the changes shown in Figures 4 and 5 with respect to the increasing distance from IP, may be due to different dispersion properties of superimposing incident and reflected waves.

Analyzing the magnitudes of reflection coefficients (CRC magnitudes) depending on frequencies $C_{r,i}(f)$, yet in [5], the author had attached limited frequency ranges to 'partial waves' (partial standing waves), possessing properties equivalent to those described above (Fig.5).

For that purpose the above formula [12] had been used.

In the following the maximum magnitudes of the reflection coefficient $C_{r,II}(f)$ (related to $E_{max,II}$ and $E_{min,II}$) of a smooth revetment are compared to those of hollow revetment elements (cf. Fig.2) both at a slope 1:3 in Figure 7. Similarly Figure 8 contains the maximum magnitudes of the reflection coefficient $C_{r,II}(f)$ of a smooth revetment and hollow blocks (cf. Fig.9) both at a slope 1:2 in Figure 8.

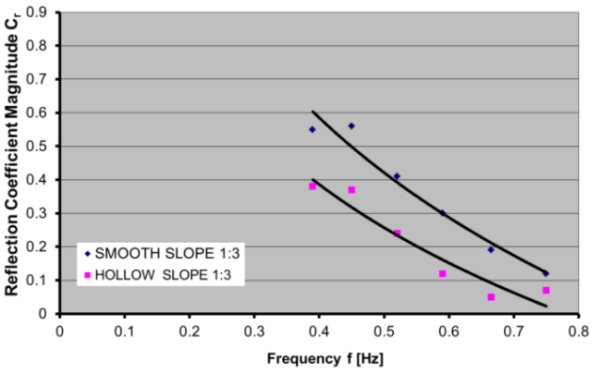

Figure 7: Spectral reflection coefficients $Cr,_{II}(f)$ of partial waves at slopes 1:m = 1:3 with mean values of the respective component frequencies f.

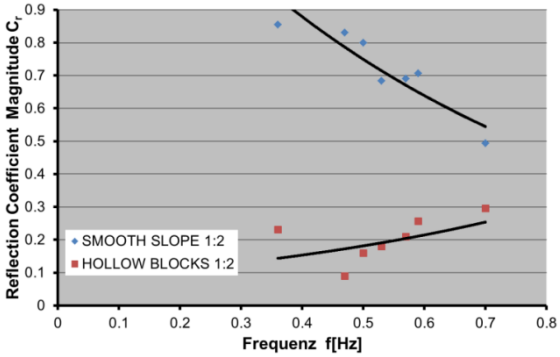

Figure 8: Spectral reflection coefficients $Cr,_{II}(f)$ of partial waves at slopes 1:m = 1:2 with mean values of the respective component frequencies f.

Table 1: Magnitudes C_r of the CRC Γ at various revetments specified in column 1.

1	2	3	4	5	6	7	8
Type	1:n	Frequency [Hz]	$_{min}C_r$	C_{rm}	$_{max}C_r$	C_r-Trend	Type of breaker
Smooth slope	1:3	$0.38 \le f \le 0.76$	0.12	0.33	0.56	decreasing	Plunging breaker
Hollow Cubes	1:3	$0.38 \le f \le 0.76$	0.05	0.20	0.39	decreasing	Collapsing breaker
Smooth slope	1:2	$0.36 \le f \le 0.70$	0.50	0.72	0.85	decreasing	Plunging breaker
Big Hollow Cubes	1:2	$0.36 \le f \le 0.70$	0.10	0.20	0.30	indifferent	undefinable

As expected the bigger reflectivity of the *smooth* revetment is confirmed for the *steeper* slope 1:2 and the *decreasing trend* of C_r with increasing frequency is found not only for the smooth slopes but also for hollow slope 1:3. It is striking, however, that there are rather low magnitudes of the reflection coefficients attached to the big hollow cubes (on 1:2) accompanied by a fairly indifferent frequency trend.

While in [3] the primary focus had been put on slope 1:3, in the present study the findings regarding the *phase* of the complex reflection coefficient at the slopes 1:2 will be discussed in detail, because of the tremendous differences between the two kinds of revetment. The respective measurements had been carried out by Lemke und Nicolai [7] while previous evaluations and conclusions had been presented by the author [8].

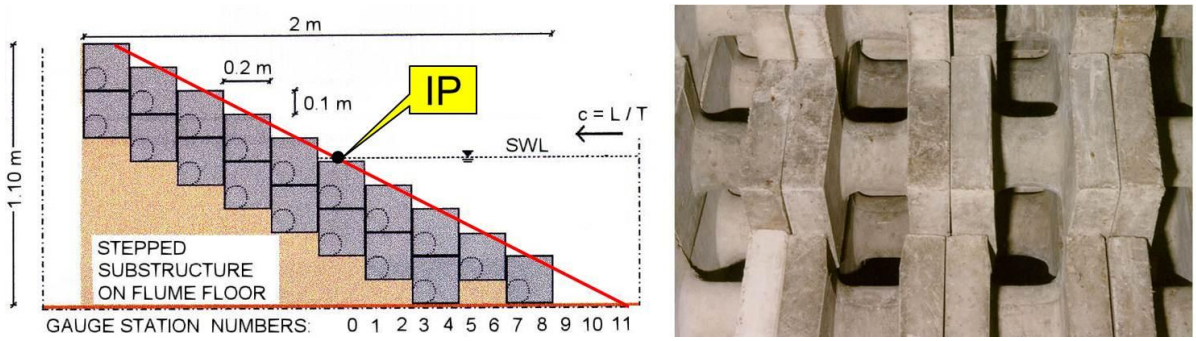

Figure 9: Sectional and cut-out views of permeable test structure inclined 1:m = 1:2.

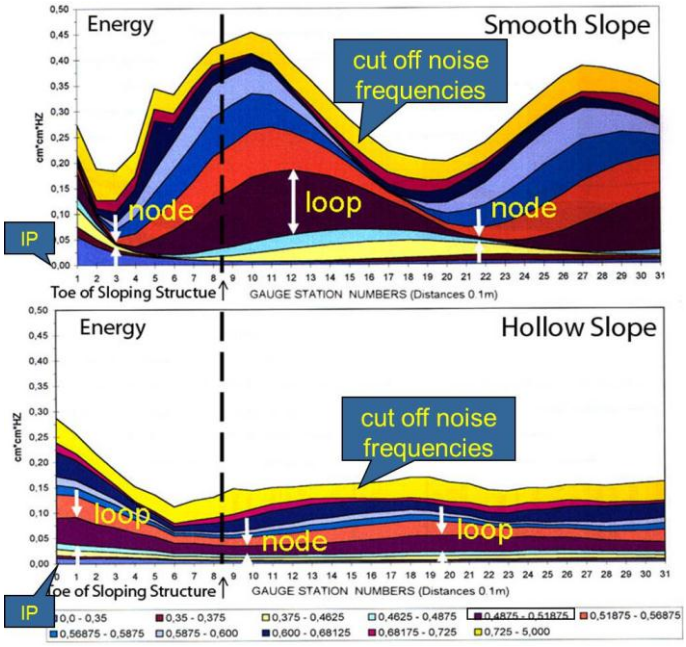

Figure 10: Energy content of 11 frequency ranges with the distance from IP. Upper part: Evidence of partial standing wave components (partial waves) assigned by distinct loops and nodes. Lower part: Evidence of partial waves containing much less energy. Both parts: Distinct phase differences $\Delta\psi$ between partial waves of same frequency ranges.

As to be seen from Figure 9, in this case two layers of a special kind of big hollow cubes had been piled up in such a way that a stepped permeable structure was formed. Corresponding to the investigations on slope 1:3, the point IP of the still water level intersecting the slope face was selected as the point of reference. Hence in this case synchronous measurements of water level deflections had been possible above the smooth slope starting at a distance of 10cm from IP and above the hollow block structure starting directly at IP. The total measurements extended up to the distance of 3.1m from the structure quasi synchronously at gauge stations intervals of 10cm. Differing from the investigations on slopes 1:3 [3] [4], in this case truncated wave sequences had been applied in such a way that re-reflection and resonance effects were excluded from the analyzed data. Instead of plotting the data of any partial wave separately, in Figure 10 the energy contents of all partial waves, comprising different component frequency ranges, appear piled up with reference to the distance from IP.

Omitting signal noise of frequencies f > 0.725 Hz (i.e. the upper yellow-orange areas in both plots), at the smooth slope, partial waves can very well be identified by their extreme values of energy, representing loops and nodes respectively. Moreover the “displacement effect” (Selective reflection, (Büsching, 1995) [6]) is very distinct for the plain slope: The lower the frequency components of the partial waves, the more downslope they are reflected with the consequence of the relative shifting to be seen in the graph.

Vice versa the nodes_I of partial waves (cf. Fig.5) get the closer to IP the higher their mean frequencies. Actually this effect had also been found for the smooth slope 1:3. In [3], however, the finding of phase shifts in the range of $\Delta\varphi \approx 180°$ had been emphasized for both smooth slopes, whereas in the following a more thorough analysis of the phase shift is intended with respect to the phase $\Delta\varphi$ of the complex reflection coefficient and with respect to the position of the partial waves in relation to IP.

Such an approach is absolutely necessary, because from Figure 10, there can not only be watched the tremendous *different* amounts of energy in front of the two slopes, but also the existence of big phase differences $\Delta\psi$ between respective partial waves.

As an example with regard to the frequency range $0.4875\text{Hz} \le f \le 0.51875\text{Hz}$ (purple), whose loops and nodes in the graph are marked by arrows, the distance of corresponding phase points is 0.70m. Applying 0.95m as the distance between node and loop (also taken from the graph) the phase difference can easily be calculated to be approximately $\Delta\psi \approx 66°$.

In contrast to the smooth slope, above the hollow structure, there is a loop documented between stations 5 and 0 due to increasing energy, see Fig.10. This increase is, however, combined with a shifting of energy from lower frequencies $0 < f < 0.46875\text{Hz}$ to higher frequencies $0.4875\text{Hz} < f < 0.725\text{Hz}$ and this is in accordance with the visual observation of high turbulent flow into and out of the hollow structure respectively. Moreover a special type of breaker could *not* be identified.

Thus it can be supposed that besides intense energy dissipation at the hollow structure, also the extent of the observed phase difference is responsible for the very low magnitudes of reflection coefficients to be found. By contrast, at a slope 1:3 a comparable phase difference with reference to the smooth slope is only $\Delta\psi = 18° < 66°$ attached to a *similar* frequency range $0.49\text{Hz} \le f \le 0.54\text{Hz}$. Although the reduction of reflection coefficients is impressive for the hollow revetment 1:3 (Fig. 7) also, the collapsing breaker occurring at that structure is rather different from the surf characteristics at the hollow cubes structure inclined 1:2.

4. Magnitude and phase of complex reflection coefficients

On the basis of the data on irregular waves contained in this article, first of all some magnitudes and phases of complex reflection coefficients are calculated in Tables 2 and 3 and are plotted in Figures 11 and 12.
For that purpose the mean values of magnitudes C_r are taken from Fig.7 and Fig.8 respectively and the wave lengths L and distances η_{max}, to be used in equation [14a], had been taken from Fig.10 for the slopes 1:2, whereas the respective data belonging to slopes 1:3 stem from Figure 5.
Additionally the data of the theoretical cases of positive and negative total reflection are shown.

Table.2: Calculation of phase $\Delta\varphi$, real part Re[Γ] and imaginary part Im[Γ] of the CRC of 5 partial waves, representing the *core* frequencies of the spectrum, at a smooth slope and at Hollow cubes both inclined 1:2, cf. Figure 11.

Type	1:n	Frequency	Wave length	η_{max}	C_r	$\Delta\varphi$	Re[Γ]	Im[Γ]
		[Hz]	[m]	[m]		[°]		
Pos. total reflection	∞				1.00	0.0	1.00	0.00
Neg. total reflection	1:n				1.00	180.0	-1.00	0.00
Smooth slope	1:2	0.475	4.40	1.40	0.83	130.9	-0.54	0.63
Smooth slope	1:2	0.503	3.80	1.20	0.80	132.6	-0.54	0.59
Smooth slope	1:2	0.544	3.40	1.00	0.68	148.2	-0.58	0.36
Smooth slope	1:2	0.578	3.00	0.90	0.69	144.0	-0.56	0.41
Smooth slope	1:2	0.594	2.90	0.80	0.70	161.4	-0.66	0.22
Hollow cubes	1:2	0.475	4.40	2.15	0.09	8.2	0.09	0.01
Hollow cubes	1:2	0.503	3.80	1.95	0.16	-9.5	0.16	-0.03
Hollow cubes	1:2	0.544	3.40	1.80	0.18	-21.2	0.17	-0.07
Hollow cubes	1:2	0.578	3.00	1.65	0.21	-36.0	0.17	-0.12
Hollow cubes	1:2	0.594	2.90	1.60	0.25	-37.2	0.20	-0.15

Table.3: Calculation of mean phase values $\Delta\varphi$, real part Re[Γ] and imaginary part Im[Γ] of the CRC of *irregular* waves acting at revetments specified in column 1 to 3, cf. Figure 12.

1	2	3	4	5	6	7	8	9
Type	1:n	Frequency	Wave length	η_{max}	C_r	$\Delta\varphi$	Re[Γ]	Im[Γ]
		[Hz]	[m]	[m]		[°]		
Smooth slope	1:3	$0.38 \le f \le 0.76$	3.65	0.73	0.33	216.0	-0.27	-0.19
Neg. total reflection	1:n				1.00	180.0	-1.00	0.00
Hollow revetment	1:3	$0.38 \le f \le 0.76$	3.65	1.00	0.20	162.7	-0.19	0.06
Smooth slope	1:2	$0.36 \le f \le 0.70$	3.5	1.00	0.72	154.3	-0.65	0.31
Hollow cubes	1:2	$0.36 \le f \le 0.70$	3.5	1.85	0.20	-20.6	0.19	-0.07
Pos. total reflection	∞				1.00	0.0	1.00	0.00

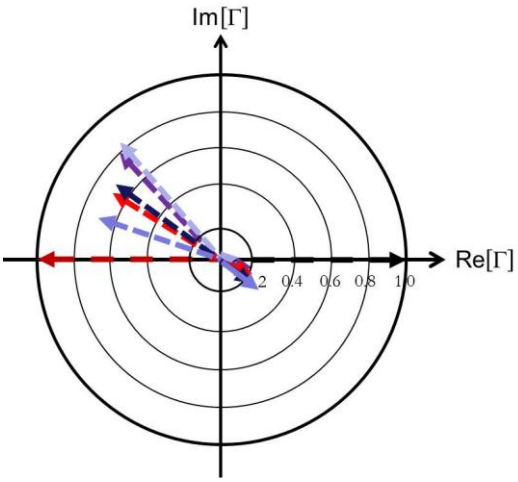

Figure 11: Phasor diagram belonging to Tab. 2

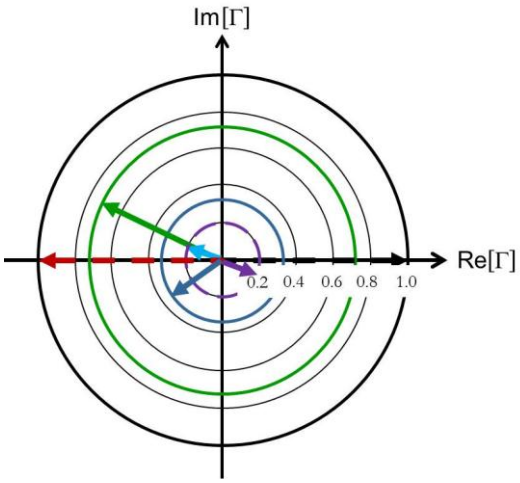

Figure 12: Phasor diagram belonging to Tab. 3

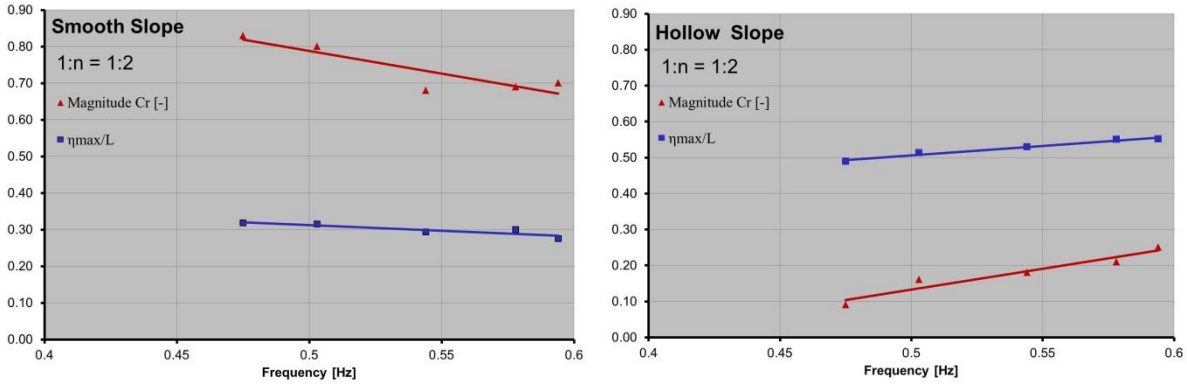

Figure 13. Magnitudes C_r and relative loop distances $\eta_{max/L}$ with frequency.

In order to consider the dependence on frequency as well in the data presentation, besides the common subdividing of complex functions into Real Re[Γ] and Imaginary Im[Γ] parts (not shown) in this case also the magnitudes C_r and the relative loop-distances η_{max}/L are plotted, see Figure 13.

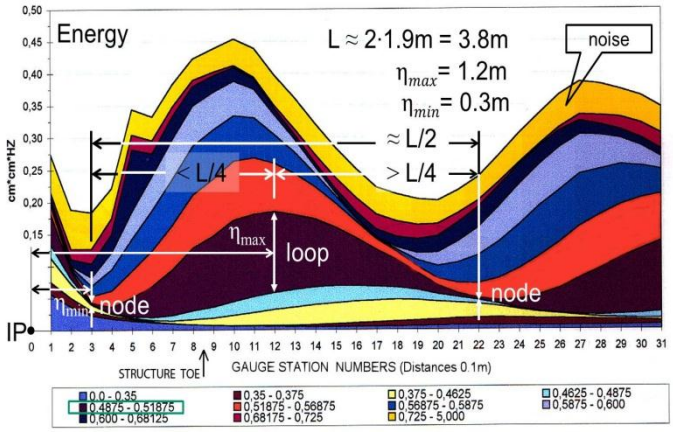

Figure 14. Horizontal wave asymmetry due to decreasing distances between loops and nodes in onshore direction, at the smooth slope.

By judging the accuracy of the data taken from charts like Figure 10, not only the measurement interval of 10cm has to be considered, but also the fact that near breaking steepening waves are deformed continuously, e.g. see Büsching (1974) [13]. The horizontal wave asymmetry is not only expressed by the above described relative shifting of the partial waves, but also by the decreasing distances between loops and nodes of all partial waves in the onshore direction. As an example, in Figure 14 the relevant data are given for the partial wave of the frequency range $0.4875\text{Hz} \leq f \leq 0.51875\text{Hz}$ (purple). Hence, the formulae [14a] and [14b] yield different results even for neighboring loops and nodes at a smooth slope. In this case $\Delta\varphi = 132{,}6° > 123{,}2°$, to be compared to the respective value in the table 2. This means that not only CRC magnitudes vary with distance from the structure (as stated by Büsching, 1992) but also the CRC phases do so.

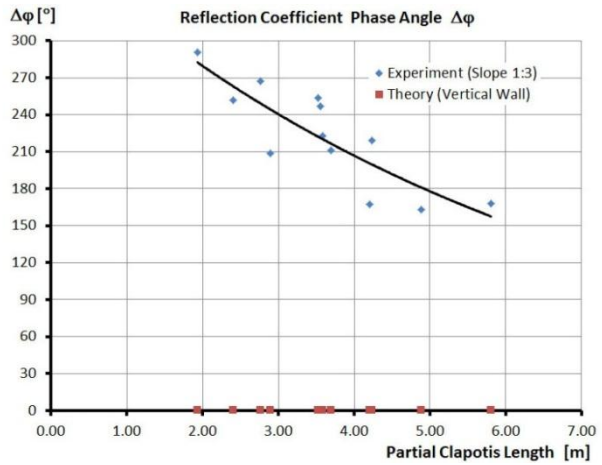

Figure 15: Phase angles of reflection coefficients of 12 partial waves at a smooth revetment of slope 1:3. Δφ converted from a/L-values taken from [3] or [4].

With respect to phase shifting at reflection, in *previous* publications the author had referred to the nearest distances '*a*' of the imperfect nodes of partial standing waves with reference to IP.

Hence, there are such values related to the wave length *a/L* as functions of the *wave length* in [9] and as functions of *frequencies* and *slope angles* in [6].

In addition to the smooth revetment 1:3, commented in detail in [3] and [4], there is a conversion from *a/L* into $\Delta\varphi$ contained in Figure 15 by applying formula [15]

$$\Delta\varphi[^\circ] = 180\,(1 - 4\,a/L) \qquad [15]$$

Furthermore at BUAS a set of investigations on *monochromatic* waves had been executed in 1995. Such had been specified by 6 frequencies in the range of 0.45Hz ≤ f ≤ 0.85Hz and by 6 slopes in the range 1:0 ≤ 1:n ≤ 1:3. The corresponding measurements referring to smooth and hollow slopes had been carried out by Thienelt und Meyer (1995)[10], whereas there is an analysis on the phase shift by the author in [6]. In this case, however, the conventional method of evaluating the water level deflections was used in connection with Healy´s (1953) formula [11] with respect to the magnitudes of the reflection coefficients, whereas a/L (with reference to IP) had been used for characterizing the phase shift.

At this place, however, the *real phase information* $\Delta\varphi$ of the complex reflection coefficient has been converted from a/L-values also by using formula [15], see Figure 16 and 17 respectively.

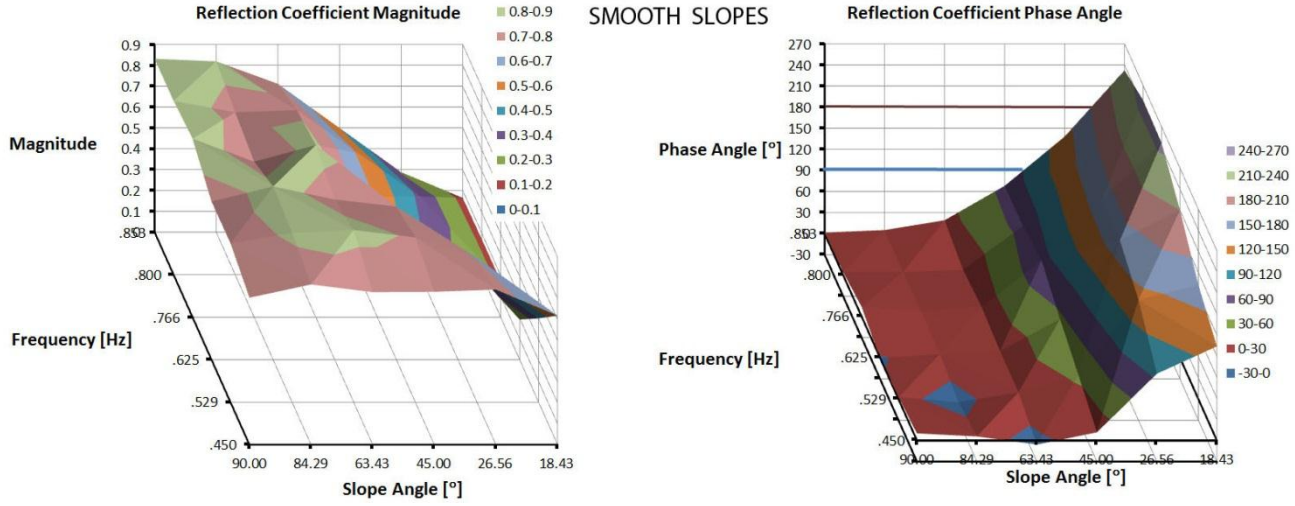

Figure 16: Magnitude (left) and phase (right) of complex reflection coefficients of 6 smooth revetments inclined 90°, 84,29°, 63,43°, 45°, 26,56° and 18,3° for monochromatic waves covering the frequency range 0.45Hz ≤ f ≤ 0.853 Hz.

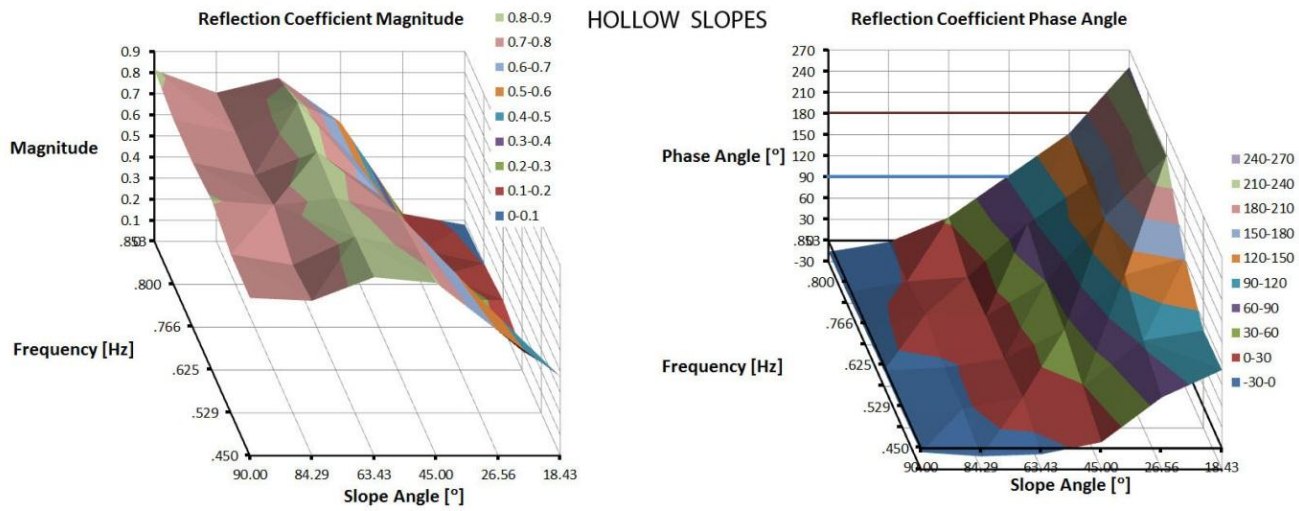

Figure 17: Magnitude (left) and phase (right) of complex reflection coefficients of 6 hollow revetments inclined 90°, 84,29°, 63,43°, 45°, 26,56° and 18,3° for monochromatic waves covering the frequency range 0.45Hz ≤ f ≤ 0.853 Hz.

5. Discussion and Outlook

Tab.2, Figure 11 Comment:

The 5 phasors of partial reflection coefficients referring to *smooth* slopes, are characterized by magnitudes of about $C_r = 0.72$ and frequencies 0.46Hz ≤ f ≤ 0.6Hz (core of spectrum). They all are in the second quadrant. Re[Γ]<0 means negative reflection, but the phase jump is much smaller than 180° and on an average also smaller than on the *smooth* revetment 1:3, cf. Figure 15.

On the other hand the phasors referring to hollow slopes with magnitudes of about $C_r = 0.2$ are nearly all in the fourth quadrant, which means positive reflection Re[Γ]>0.

Tab.3, Figures 12 and 15 Comment:

At this place the phasors belonging to the revetments inclined 1:2 and 1:3 are compared as specified in the table. On the one hand the *mean values* resulting from Figure 11 are shown, and on the other hand especially for the *smooth* revetment 1:3 the mean phase value from Figure 15. The later phase value of $\Delta\varphi = 216°$ is in the same order as calculated from Tab. 3 according to Figure 4. By this reason in this case the phasor is in the third quadrant, while the phasor belonging to the hollow slope 1:3 is still in the second quadrant.

Comparing the complex reflection coefficients of the *two hollow structures* on slopes 1:2 and on 1:3, it is worth mentioning that apparently there is a big difference in the mode of hydraulic action: Because of the equal magnitudes $C_r = 0.2$, this is, however, expressed only by the big phase difference of about *180°*.

Figures 16 and 17 Comment:

Comparing the presentations of the magnitudes C_r and the phases $\Delta\varphi$ of the CRCs, it is striking that

- there is an opposite trend between magnitudes and phase angles with respect to the slope angle axis, while the phase angles increase with decreasing slope angles and
- there is also an opposite trend between magnitudes and phase angles with respect to the frequency axis at least for slope angles 1:3 ≤ 1:n ≤ 1:1 (18,43°≤ α ≤ 45°), while the phase angles decrease with decreasing frequencies f (or increasing wave lengths L respectively).

The extrapolation on a bigger frequency range and on even flatter slope angles leads to the following result:

The partial reflection between the two distinguished poles of positive and negative *total* reflection is characterized by combined trends describing

- that the *shorter* the waves are and the *flatter* the slope angles, there is a *stronger* tendency on negative reflection and even for $\Delta\varphi>180°$,
- that the *longer* the waves are and the *steeper* the slope angles, there is a *stronger* tendency on positive total reflection and even on the tendency of a broken Clapotis and
- that the *longer* the waves are and the *flatter* the slope angles, there is a *weaker* tendency on negative reflection ($\Delta\varphi<180°$).

The significant conditions of positive and negative *total* reflection of course cannot even be found for *smooth* slopes. The proper approximation to the paired values ($C_r = 1$, $\Delta\varphi = 0°$) appear, however, more distinct than to the paired values ($C_r = 1$, $c = 180°$).

Attempt to classify breaker types by defining ranges of phase angles.

In [6] the author´s previous attempt to classify breaker types on smooth and hollow revetments had also been based on the relative distances *a/L* of the imperfect nodes of partial standing waves nearest to the structure. As the respective survey had been compiled, however, by *visual observations* provided by *several* individuals, a reservation may be imposed on its results. Nevertheless the result, converted by equation [15] to the phase angles $\Delta\varphi$ of the reflection coefficient, is given in Tab.4 for the respective frequency range.
Accordingly the effect of the hollow revetment versus the smooth revetment is not only expressed by *smaller magnitudes* of the reflection coefficients on slopes 1:m $\leq$ 1:1 ($\leq 45°$), but also by a *different* reference of phase angles and breaker types. Bigger phase angles are needed for the formation of *comparable* breaker types on hollow slopes than on smooth slopes.
It should be emphasized, however, that *plunging* breakers exist on the smooth slope 1:3 at all frequencies, but this type of breaker actually could not at all be observed on the hollow slope structures.

Table 4: Phase angle ranges of complex reflection coefficients assigned to breaker types observed at smooth and hollow revetments [6].

Smooth slope	Phase angle limits [°]			Hollow slope	Phase angle limits [°]	
	min $\Delta\varphi$	max $\Delta\varphi$			min $\Delta\varphi$	max $\Delta\varphi$
nearly perfect Clapotis	0	36		nearly perfect Clapotis	-14	72
transition to surging	36	72		transition to surging	72	108
surging breaker	72	108		surging breaker	108	144
collapsing breaker	108	162		collapsing breaker	144	252
plunging breaker	162	252				

Alternatively a rough classification basing merely on the phasors of Figure 12 are given in Table 5.

Table 5: Observed breaker types assigned to phase angle ranges derived from the phasors of Figure 12.

Phase angle $\Delta\varphi$	Type of breaker	Additional phenomenon
$\approx 0°$	broken Clapotis	super critical steepness
1st or 4th quadrant	no distinct breaker type	dissipation>transmission
$\approx 180°$	surging breaker	low dissipation
2nd or 3rd quadrant	collapsing or plunging breaker	dissipation and transmission

Accordingly distinct positive reflection assigned by $\Delta\varphi \approx 0°$ and super critical wave steepness could be attached to a broken Clapotis, whereas distinct negative reflection assigned by $\Delta\varphi \approx 180°$ most likely could be attached to a surging wave.
The more, however, $\Delta\varphi$ differs from 180°, the more likely partial standing waves will occur accompanied by collapsing or plunging breakers - together with dissipation and run up (transmission).
Contrary, at weak positive reflection, assigned by $\Delta\varphi$ in the first or forth quadrant, the dissipation is likely more intense than transmission.
Finally it can be stated:
As the CRC phase angle controls the positioning of the partial standing wave and thus the location of the breaker depth at a slope, its necessity for the complete description of the wave breaking is obvious and therefore it should be considered at future large scale investigations. Nevertheless it should be emphasized that due to the small sample size, general conclusions on the breaker type depending on the kind of reflection cannot be given at present.
On the other hand such results can be expected in future, if targeted investigations will not only be oriented on the magnitudes but also on the corresponding phase data of complex reflection coefficients, - *both* maybe related to Irribarren numbers.
In doing so, especially the nature of the large scatter within the magnitudes C_r of the reflection coefficients with respect to Irribarren numbers $0.3 \leq \xi \leq 9$ (van der Meer, 1988) [11] possibly can be clarified.
The use of complex reflection coefficients is another example of phenomena known from electromagnetic or other kinds of waves, having particular significance on water waves too.
It may be speculated that an all-in approach of corresponding complex coefficients on *reflection, transmission and absorption* could be useful.

References

[1] SCHOEMAKER, H.J. AND J.TH. THIJSSE: 'Investigation of the reflection of waves', *Third Meeting, Intern. Assoc. Hyd. Structures Res.*, 1-2 September, 1949
[2] SUTHERLAND , J. AND O'DONOGHUE, T.: 'Wave Phase Shift at Coastal Structures', *Journal of Waterway, Port, Coastal and Ocean Engineering*, Vol. 124, No. 2, March/April, 1998, pp. 90-98.
[3]BÜSCHING, F.: ‚Phasensprung bei der partiellen Reflexion irregulärer Wasserwellen an steilen Uferböschungen', 1. *HANSA – International Maritime Journal* - C 3503 E, 147, H.5 p.87-98, 2010 (fehlerhafter Druck). 2. *BINNENSCHIFFFAHRT* - C 4397 D, 65, H.9 p.73-77 & H.10 p.64-69, 2010.
[4]BÜSCHING, F.: 'Phase Jump due to Partial Reflection of Irregular Water Waves at Steep Slopes', 1. *Coastlab 10*, Barcelona, Spain, 28th-30th September, 1st October 2010, Paper No. 67, p.1-9. 2. *PowerPoint*, urn:nbn:de:0066-201011165http://hydromech.de/Veroeff/phase_jump_20101116.pdf , 25 slides
[5] BÜSCHING, F.: 'Wave and Downrush Interaction on Sloping Structures', Proc. *10th International Harbour Congress*, Antwerpen, S. 5.17-5.25, 1992
[6] BÜSCHING, F.: 'Hollow Revetment Elements', 1. Proc. *Fourth International Conference on Coastal and Port Engineering in Developing Countries COPEDEC IV*, Rio de Janeiro, S. 961-976, 1995. 2. *Beiträge aus dem Küsteningenieurwesen* (Papers on Coastal Engineering), FH Bielefeld, Abt. Minden, Nr. 4, 1996
[7] LEMKE, S. UND NICOLAI, A.: ‚Reflexion an einer aus Beton-Hohlformkörpern (Hollow Cubes) bestehenden Böschung mit der Neigung 1:2', *Diplomarbeit FH Bielefeld University of Applied Sciences*, 1998, unveröffentlicht.
[8] BÜSCHING, F.: 'Reflection from Hollow Armour Units', Proc. *COPEDEC V*, p.1362 - 1370, Cape Town, South Africa 1999.
[9] BÜSCHING, F.: 'Combined Dispersion and Reflection Effects of Sloping Structures', 1. *4th International. Conference on Coasts, Ports and Marine Structures, ICOPMAS* 2000, Proceedings

(Abstract and CD), Bandar Abbas, Iran 21.-24. Nov. 2000. 2. *International Conference on Port and Maritime R&D and Technology ICPMRDT*, p.411-418, Singapore, 29.-31.10.2001, Proc./ CD.

[10] MEYER, O. UND THIENELT, W.: ‚Partiell stehende Wellen an unterschiedlich geneigten Böschungsbauwerken', *Diplomarbeiten FH Bielefeld University of Applied Sciences*, 1995, unveröffentlicht.

[11] VAN DER MEER, J.W.: 'Rock slopes and gravel beaches under wave attack'. *Doctoral thesis. Delft University of Technology*, 1988. Also *Delft Hydraulics Communication No. 396*.

[12] MANSARD, E.P.D. AND E.R. FUNKE: 'The Measurement of Incident and Reflected Spectra Using a Least Squares Method'. *17th International Conference on Coastal Engineering,* Sydney, 23-28 March, 1980.

[13] BÜSCHING, F.: ‚Über Orbitalgeschwindigkeiten irregulärer Brandungswellen', *MITTEILUNGEN DES LEICHTWEIß-INSTITUTS FÜR WASSERBAU DER TU BRAUNSCHWEIG*, H.42, P. 0 - 256, 1974.

[14] BÜSCHING, F.: 'Complex Reflection Coefficients Applied to Steep Sloping Structures', 1. *Coastlab 12*, Ghent, Belgium, 17-20 September, 2012. 2. PowerPoint Presentation, http://www.digibib.tu-bs.de, in printing.